Fractal morphology of the flickering of the cataclysmic variable star KR Aurigae

Ts. Georgiev[1,2], A. Antov[1], R. Bachev[1], S. Boeva[1],
G. Latev[1], B. Spasov[1], K. Stoyanov[1], S. Tsvetkova[1]
[1] Institute of Astronomy and Rozhen NAO, 1784 Sofia
[2] New Bulgarian University, 1618 Sofia
tsgeorg@astro.bas.bg
(Submitted on 9.10.2011; Accepted on 25.02.2012)

Abstract. We apply fractal analysis on 29 light curves of KR Aur in the system UBVRI, 20 in high brightness light state and 9 in low state. The method has been tested on normal and uniform random processes, on light and colour curves of SN 2007gh, on the Sun spot numbers and on the flickering of the cataclysmic variable V425 Cas. The brightness of KR Aur is 13-18 mag, the monitoring time is 1-10 hours and the single exposure time is 0.5-5 min. Two fractal dimensions, based on the local amplitudes (MAX-MIN), $1.2 < D_1 < 2.9$, and standard deviations (RMS), $1.5 < D_2 < 1.9$, have been estimated with accuracy $\approx 5\%$. Different fractal dimensions for minute time-scale (7-30 minutes) and hour time-scale (0.5-5 hours) were found, both for high and low state, in all bands. The first main result is that the flickering of KR Aur appears at least bi-fractal, with two moderate varing fractal dimensions and typical dividing time ≈ 30 min. The influence of the observing parameters on the estimation of the fractal dimensions is elucidated. Further, the levels of the fractal parameters at time scales 10 min and 100 min have been used to show that the relative amplitudes and standard deviations of the flickering in low state, when the mean total flux is ≈ 100 times fainter, occurs about 3 times higher. However, because of the large single exposure time, 5 min in low state, this distinction is underestimated. The second main result is that the relative flickering energy in the low state is significantly higher than the high state.

Key words: cataclysmic stars: flickering, fractal analysis: data rows

Introduction

KR Aurigae has been discovered as a peculiar variable by Malina Popova (1965). It is a binary system consisting of a white dwarf and a red dwarf stars with orbital period of 3.907 hours (Shafter, 1983). The contemporary distance to this object is estimated to be about 1200 pc (Boeva et al. 2010), corresponding to absolute magnitude at high state 3.0–3.5 mag. The apparent V-magnitude of the system is about 14 mag at high state and about 19 mag in low state.

KR Aur is classified as a nova-like cataclysmic variable (CV) of VY Scl type (anti-dwarf nova). In normal (high) state such system accretes at high mass transfer rate. At random intervals deep dips occur lasting from days to years, suggesting that most or even the whole of the accretion disk disappears during the low state.

The brightness of the CVs varies on minute-to-hour scale with amplitude of a few tenths of a magnitude. This variation is called usually "flickering". As a result of multitude observations in B, V and I bands, Boeva et al (2007) established that in log-log scale the amplitude of short scale flickering ΔF is proportional to the mean flux F: $\log\Delta F = k \times \log F + \text{const}$, with $k = 0.70 - 0.75$.

Recently Bachev et al. (2011) studied the character of the flickering of KR Aur on intra-night time scales using different statistical methods. Using the

auto-correlation function for 4 light curves they found that the correlation times are 30 – 100 min. Based on the cross-correlation function between I and V band they found no conclusive evidence of inter-band time delays exceeding 30 sec. Using the structure function in 4 cases they gave preference to accretion disk instability models, not for shot-noise driven variability (when the variations are due to many independent, explosive events). They found also that for time intervals of 10-10 min the light curves show predominantly slow inclines and sharp declines, i.e. as in the disk-instability models. At the end, they searched for signatures of low-dimensional chaos and considered no clear indications of such one.

Generally, Bachev et al.(2011) conclude the variability on time scales of 10-100 min is mostly due to evolving disturbances, traveling perhaps from the periphery to the center of an accretion disk. Shorter variations, on scales less than 5-10 min, appear to be predominantly stochastic in nature.

In the present study we apply the simplest fractal methods, based on the local amplitudes and RMS in 1D data row. The goals are (i) to characterize and classify the morphology of the flickering curves in high and low states by their fractal dimensions and (ii) to characterize and compare the energy of the flickering in high and low states.

Section 1 presents the observing material. Section 2 describes the used fractal indicators, parameters, plots and dimensions. Section 3 presents the gallery of 29 light curves and respective fractal plots, shown in the Appendix (Fig.10-16), as well as a classification of the flickering curves by means of two fractal dimensions. Section 4 shows the influence of various observing circumstances on the fractal dimension. Section 5 presents the anti-correlation between the mean flux of the system and the relative flux of the flickering. Section 6 summarizes the main topics and the results of this study.

1 Observations and photometry

This study is based on UBVRI CCD observations carried out with the 60cm Cassegrain reflector of Belogradchik Observatory, Bulgaria, as well as with the 60 cm Cassegrain reflector, the 50/70 cm Schmidt camera and the 2 m RCC telescope of the Rozhen NAO, Bulgaria. The observational log with appropriated by us observation identifiers is presented in Table 1. The light curves and the respective fractal plots are presented in the Appendix. The numerical results are displayed in Tables 2, 3 and 4.

The observing material includes 29 high-quality intra-night light curves. Among them 20 present the object in a high state, with $m_V \approx 14$ mag and 9 corresponds to a low (and intermediate) state, with $m_V \approx 18$ mag. Various time series of observations were used. The duration of the observations are 1-10 hours, the number of the single brightness points are between 21 and 549, the single exposures are between 30 and 300 s.

After flat field and dark current corrections of the frames, the aperture magnitudes of the stars were extracted and calibrated through standard stars in the field, and the light curves were built. The standard photometric errors in the high state of the object is about 0.01 mag and in the low stage about 0.02 magnitudes, while the amplitudes of the magnitude variations of the flickering rows lie in the interval 0.24-1.41 mag. We consider the precision of

our data to be high enough for a successful application of the fractal analysis, described below.

2 Fractal indicators, parameters, plots and dimensions

The intra-night flickering of the cataclysmic and symbiotic variables appears chaotic on time-scales from seconds to hours and the astronomical time series are usually not equally sampled. Many methods for time series analysis exist, but the fractal analysis, applied below, is chosen because we consider it is (i) weakly sensitive to the non equality of data sampling and (ii) simple (at least conceptually).

The fractal analysis is a tool for characterizing the self-similarity of the apparent chaos at various time or space scales. The fractal dimension, introduced conclusively by Mandelbrot (1982), is an objective measure of such self-similarity and it is useful in the studies of very different objects: complicate planar curves (land coasts and borders, Brownian motions), elevation profiles or time series (market prices, solar and geomagnetic data rows), fracture surfaces, geometry of planar objects (drainage basin of rivers, atmosphere and interstellar clouds, islands, solar grains) and even of the galaxy distribution in the Universe.

The methods applied here are based on the recommendations in the monographs of Mandelbrot 1982, Peitgen et al. 1992, Russ 1994, Hastings & Sugihara 1995, Falkoner 1997 etc. We apply the simplest 3 fractal methods, characterizing the "jagness", the "roghness" and the "periodicity" of the time series.

Let us consider a time series $\{T_i, Z_i\}, i = 1, 2, , N$, with a total length $T_T = T_N - T_1$ and mean time-sampling interval $\epsilon T = T_T/N$. Let connect the data points by straight lines to form a continuous elevation profile (Fig.1). Finally, let have a fixed position of a scanning time interval (data window) with size δT ($\epsilon T < \delta T < T_T$), with bounds T1 and T2 and with respective interpolated values in the window edges Z1 and Z2 (Fig.1).

The simplest indicators of the jagness (or of the vertical data scatter) for every fixed position of the window are (i) the maximal internal amplitude ($Z_{max} - Z_{min}$), (ii) the standard deviation Z_{rms} and (iii) the edge amplitude $|Z_1 - Z_2|$. Then we normalize them through the mean value in the interval Z_0 and use the relative **fractal indicators** (Fig.1)

(1.1) $h_1 = (Z_{max} - Z_{min})/2/Z_0$,
(1.2) $h_2 = Z_{rms}/Z_0$,
(1.3) $h_3 = |Z_1 - Z_2|/2/Z_0$.

Here h_2 is the conventional proxy of the "RMS-roghness" of the data, while h_1 is the characteristic of the largest deviations and h_3 occurs an indicator of a periodicity of the data. The values of h_1 and h_3 are divided by 2 for compatibility with h_2. In fact, $h_3 \times 2$ lies in the base of the *structure function*, used for studies of time series and used by Bachev et al. (2011).

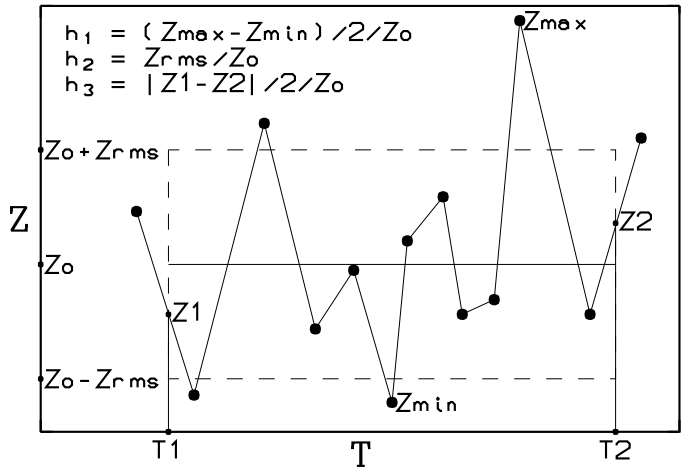

Fig. 1. A part of an arbitrary time series (dots) where the data window is placed currently between moments T1 and T2, defining 3 fractal indicators of the scatter: h_1, h_2 and h_3. The horizontal lines present the mean value Z_O and the $Z_O \pm 1Z_{RMS}$-band.

Further these indicators are used for calculation of the respective **fractal parameters** of the local scatter. Each of them is a mean value for multitude positions of the time window:

(2) $H_k(\delta T) =< h_k >, k = 1, 2, 3.$

There are two practical ways for deriving the fractal parameters (Eq. 2). First, we can divide the full duration of the time series sequentially into $1, 2, ..., m, ...$ equal parts, applying in every dividing case $1, 2, ..., m, ...$ times the window with respective size $\delta T_m = T_T/m$ and average the results for every window. Second, we can design a system of windows with uniform distribution along log δT, scan the time series with each such window (applying a suitable step, f.e. compatible with ϵT) and average the results for every window. Our preliminary investigation suggested that we should apply the second method as a better one, because it produces numerous equally sampled points on the fractal plots (Eq.3, Fig.2, 3, ...).

The parameters (2) characterize the fractal self-similarity of the "jagness" at different scales δT by different ways. Usually $H_1 > H_2 > H_3$ and when δT increases these parameters increase too. In very chaotic cases, f.e. in time series of random numbers, these parameters generally tend towards constants (see Fig.4).

Alternative (classic) fractal parameters are the sums $S_k = \sum h_k = H_k \times m$, that are sums of the vertical lengths of the time series elevations. The case $k = 1$ corresponds to the general "box-counted method" and the case $k = 3$ presents the method of Richardson, reduced to the 1D case as sum of vertical segments only. Then usually $S_1 > S_2 > S_3$ but when δT increases, these parameters decrease. Our preliminary investigation suggested that we

should apply the averaged normalized parameters (2) as better, because their intersepts do not depend on the length of the time series. (In the original application of the method of Richardson the fractal parameter can only be a sum and then the intersept of the fractal plot depends directly on the length of the coastline.)

Further, the fractal analysis of the apparent chaos in the case of time series (or elevation profile) is based on the dependences between the time window δT and the fractal parameter H_k in log-log coordinates, called **fractal plots**.

Note that here the fractal plot for H_3 is a simple version of the *structure function* (see f.e. Bachev et al. 2011). Like the stucture function, the fractal plots of H_1 and H_2 in log-log scale might have plateaus at shortest and largest δT, as well as quasi linear part between the plateaus. Let us present the linear part of the fractal plot, that can be derivad by a regression, as

$$(3)\ \log H_k = a_k + b_k \times \log(\delta T), k = 1, 2, 3.$$

In the case of time series (or elevation profile) the **fractal dimensions** are derived by definition through the slope coefficients b_k as

$$(4)\ D_k = 2 - b_k, k = 1, 2, 3$$

In the alternative case when the fractal plots are based on the sums S_k we should have fractal plots of the type $\log H_k = a_k + b_k \times \log(\delta T), k = 1, 2, 3$. Then the same fractal dimensions may be derived, however calculated as $D_k = 1 - b_k$.

The random processes, as well as the 1D Brownian motion, are known as **edge examples of extremely chaotic time series** (elevation profiles). They are characterized theoretically by the maximal fractal dimensions, $D_k = 2$. The entirely smooth curves are known as **edge examples of completely smooth time series** (elevation profiles). They are characterized theoretically by the minimal fractal dimensions, $D_k = 1.0$. In practice, the case $1.5 < D_k < 2.0$ ($0.5 < b_k < 1.0$) is interpreted as domination of fluctuations with random powers and durations, while the case $1.0 < D_k < 1.5$ ($0.0 < b_k < 0.5$ is regarded as domination of large scale trend(s).

In this study we build 3 fractal plots (3) and use 2 fractal dimensions (2), D_1 and D_2, corresponding to the parameters H_1 and H_2. Our investigation points out that the value of D_3 (derived through H_3) is strongly fluctuated and useless as fractal dimension. However, the local minimuma of the $logH_3$-plot are good indicators of the quasi periodicity in the time series, so we show the behaviour of $\log H_3$ too.

Due to the particularities of the observed time series, the values of the fractal dimensions D_1 and D_2 differ. It is important to note that D_1 is larger when high jags (simple and complicated, positive and negative) are present in all time-scales. On the other hand D_2 is larger when the local RMS-roughness is generally high in all time-scales. Usually we have $D_1 < D_2$.

Figure 2, top, presents examples of random processes, i.e. time series, derived from random numbers with normal or uniform distribution (729 data points in each series). The fractal lines are in the range 12 - 320 data points. The averaged fractal dimensions (means of D_1 and D_2) are $\approx$1.85 and $\approx$1.98

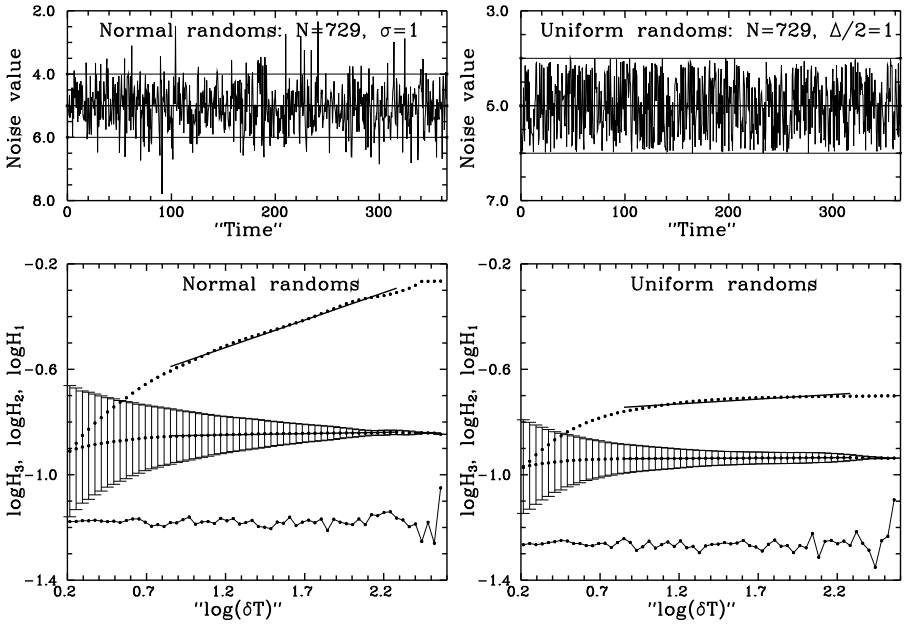

Fig. 2. Top: Random data rows derived by generators of normal (left) and uniform (right) numbers (729 data items in each series). Bottom: The fractal plots and their linear regressions (of the type of Eq.3) in the ranges of time intervals 12 - 320 data points. The individual error bars are shown only for the parameter $logH_2$. The fractal dimensions are given in Table 2.

(Table 2). In these edge cases when the data number increases to infinity the slope coefficients of the fractal plots (3) become close to zero and the fractal dimensions approach 2. Figure 2, bottom, shows the fractal plots of the examples, given in the top of Fig.2.

Figure 2, bottom-left, shows the important particularity of the normal random process – ongoing growth of the fractal dimension D_1. The reason is that the probability of large deviations increases with increasing of δT. Otherwise, in the case of the uniform random process (Fig. 2, bottom-right), the maximal deviation is limited and the D_1 rapidly approaches 2.

Figure 3 presents the V-magnitude and (B-V)-colour curves of the supernova SN 2007gh (data from Hunter et al. (2009), Dimitrov et al. (2011)). These curves are characterized by fractal dimensions $\approx$1.25 and $\approx$1.5, respectively (Table 2).

The jagness of the magnitude and colour curves of the supernova is due to photometry errors, which develop themselves mainly at the most short time scales. By these reason at short δT the plots tend to horizontal lines, like in the cases of random time series in Fig.2. On the contrary, at long δT these curves posses some large scale shapes and the respective slope coefficients grow up like for smooth curves.

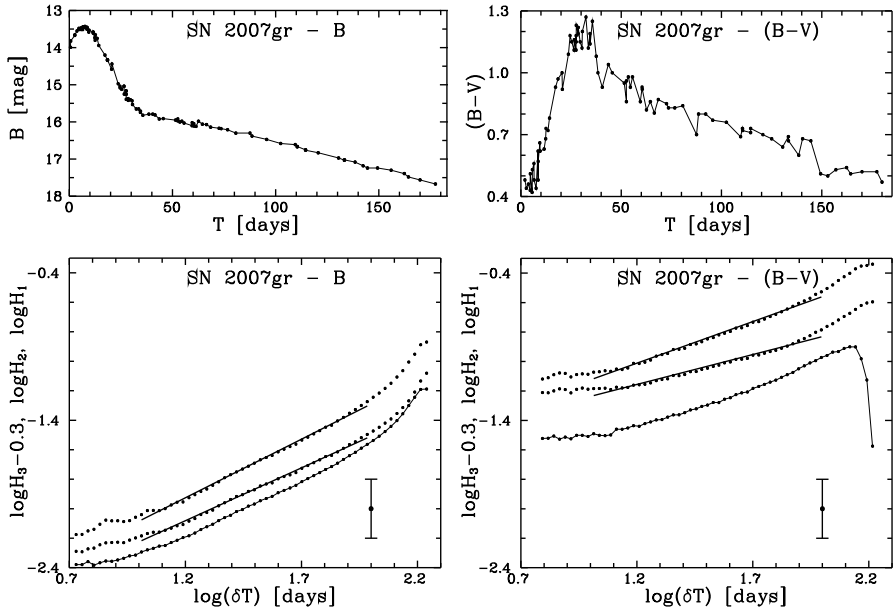

Fig. 3. Top: The magnitude (left) and colour (right) curves of the supernova SN 2007gh (Hunter et al. 2009, Dimitrov et al. 2011). Bottom: fractal plots, where parts of them are fitted by regression lines. The fractal dimensions are given in Table 2.

Figure 4 shows two very different data rows - the international monthly Wolf's numbers of the Sun spots (559 data) and a flickering row of the cataclysmic variable V425 Cas in I band (161 data, 10 s exposure times, from Tsvetkova & Boeva, 2009).

The fractal plots of the Wolf's numbers (Fig.4, bottom-left) show clearly two linear parts, corresponding to year-scale variations, 1.2-8.0 years, and decade-scale variations, 8-46 years. Such bi-fractal is interpreted as evidence that at least two physical processes cause the observed fluctuations in the data row. The year-scale variations have intermediate fractal dimension, $\approx$1.65, while the decade-scale variations show high fractal dimension, $\approx$1.95. (Table 2). Note that in contrast to the case of the supernova (Fig.3) here multitude convex details in the large scale behaviour of the curve causes increase of the fractal dimension.

Note also that in the case of the Wolf's numbers (Fig.4, bottom-left) the minima of the log H_3 curve are very good period indicators. The minima correspond to periods of 10.9 years and the 2 and 3 fold multiple periods of 21.8 and 32.7 years. However, the bends of the log H_1 and log H_2 plots lie at shorter time scales, between 7 and 9 years. We can not explain this discrepancy.

Figure 4, bottom-right, shows the fractal plots for the cataclysmic variable V424 Cas in I-band. According the plots of log H_1 and log H_2 two time scales are evident here, 2-7 and 7-40 minutes. The fractal dimensions are

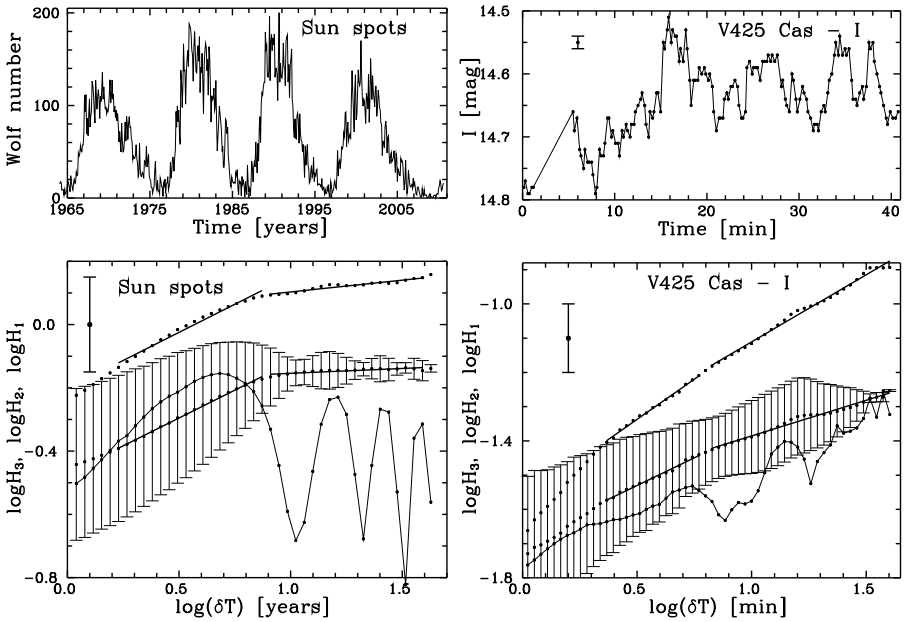

Fig. 4. Top: Monthly Wolf numbers of the Sun spots (left) and a flickering curve of the cataclysmic variable V425 Cas (right, from Tsvetkova & Boeva, 2009). Bottom: The fractal plots and linear regressions of chosen parts of them. The individual error bars are shown for the parameter $logH_2$. The fractal dimensions are given in Table 2.

$\approx$1.6 and $\approx$1.7, respectively. The standard errors are $\approx$ 0.03, so we consider this flickering bi-fractal. Note that the plot of H_3 shows quasi-periods with durations about 9 and 18 minutes.

Figure 5 presents the flickering with identification No.21B ("B" means B-band, see Table 1). Two possibilities of the flickering presentation are shown – by single data points, corresponding to the middle moments of the exposures (top-left) and by horizontal segments, limited by the beginning and the ends of the exposure (top-right). In the second case, labeled by 21B', the time scale of the graph is expanded 2 times and only the first half of the graph is presented. The fractal dimensions, corresponding to these two presentations of the light curves of the flickering, especially D_1, occur different (Table 2). Our preliminary investigations show that the first presentation is preferable as simpler and closer to the ordinary time series. The fractal plots in the Appendix and the fractal dimensions in Table 2–4 correspond to the left part of Fig.5.

3 The flickering on the diagrams D_1 – D_2 and (D_2-D_1) – D_1

The relative deviations H_1 (based on the local amplitudes in the plot) and H_2 (based on the local RMS in the plot) give estimations of the relative energy

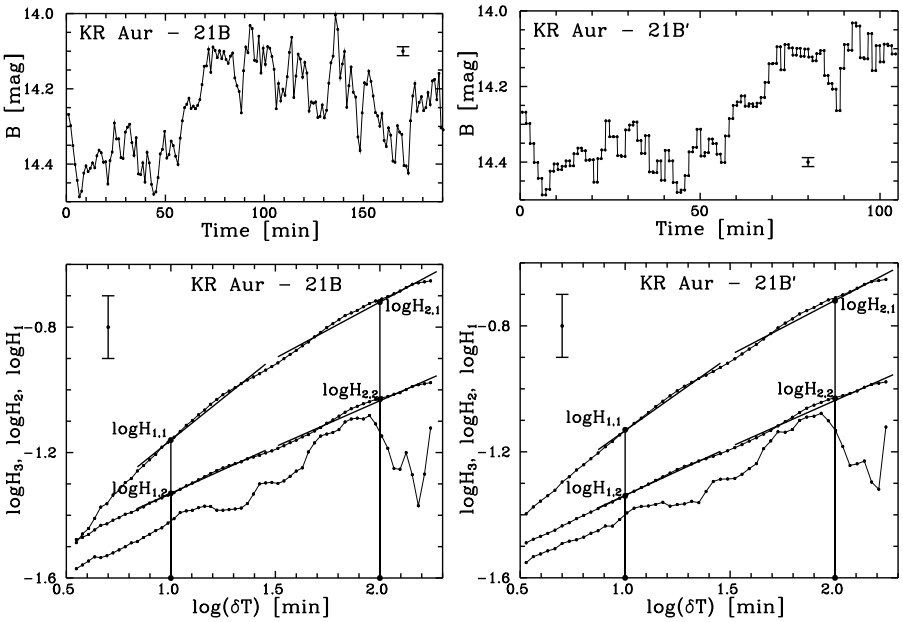

Fig. 5. Top: Two kinds of the presentation in the case of the observation No.21V – by single points, corresponding to the middle moment of the exposure (left) and by double points, corresponding to the beginning and the end of the exposure (right; only the fist half of the graph extend is shown under 2 fold abscissa enlargement). Bottom: The fractal plots and the regression lines of their parts. The fractal dimensions are given in Table 2. The vertical lines show the levels of log H_1, and log H_2, used in Section 5, Fig.9.

of the flickering. In the present study we use as energy indicators the values of H_1 and H_2, corresponding to $\log(\delta T) = 1$ ($\delta T = 10$ min) and $\log(\delta T) = 2$ ($\delta T = 100$ min).

The vertical lines in Fig.5, bottom, show the levels of log $H_{1,1}$ and $H_{2,1}$, used to characterize the relative power of the emission fluctuations at time scale of 10 minutes. The values of $H_{1,2}$ and $H_{2,2}$, characterize the same at time scale of 100 minutes. The respective data are given in Table 3 and Table 4. They are used in Section 5, in Fig.9.

Except the flickering No.21B, shown in Fig.5, the Appendix presents 28 other flickering observations of KR Aur. The flickering curves are shown in magnitudes, while the fractal characteristics are given in units $10^{-21} W/cm^2/A$. The photometric constants are taken from Bessel (1979).

Having found that the flickering of KR Aur should be regarded at least as bi-fractal, we derive the fractal dimensions for two time ranges: 7-30 minutes and 30-300 minutes. The values of the derived fractal dimensions lie in the range 1.3–1.9, with standard errors 5-10 %. (Table 3, Table 4).

The exposure times of the observations of KR Aur in high state are usually 60 s and in the low state usually 300 s. In the low state, when the data set is not long enough, we omit the hour-scale range. When the data set is not

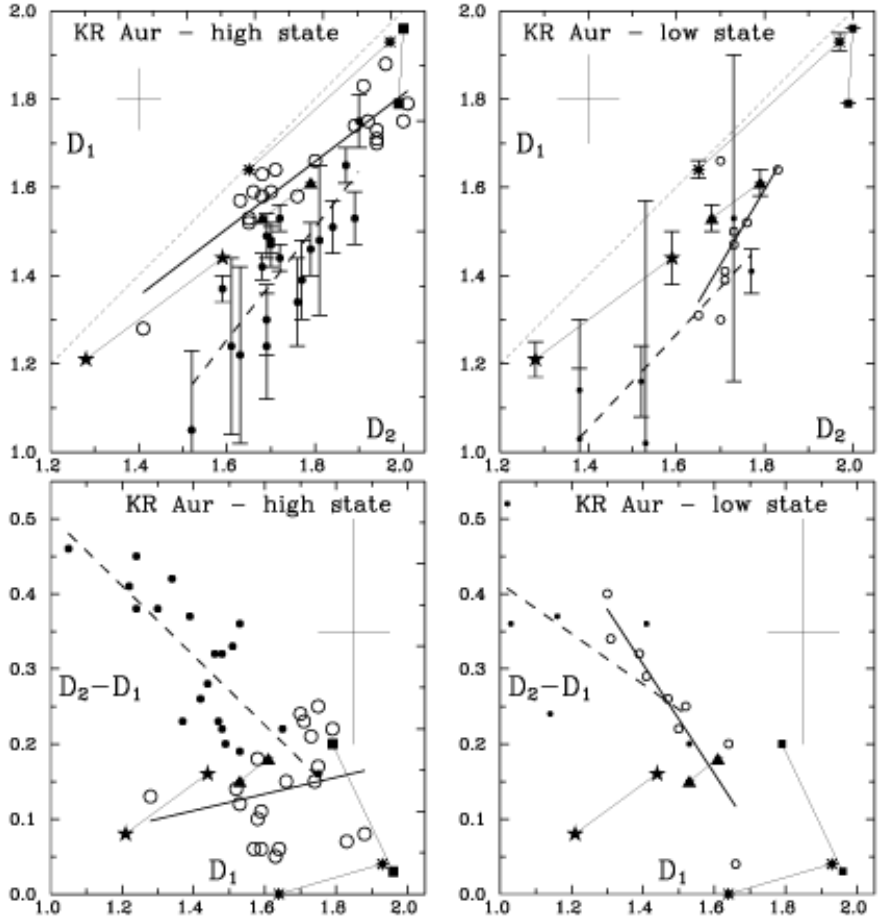

Fig. 6. Sequences of derived fractal dimensions on the diagrams D_1 - D_2 (top) and (D_2-D_1) - D_1 (bottom) for high state (left) and low state (right). Dots and dashed regression lines present the minute scale flickering (7-30 min). Circles and solid regression lines present the hour scale flickering (30-300 min). Some individual standard errors are shown. The crosses show typical standard errors. The pairs of test objects are presented here connected by thin lines, as follows: squares - random processes (Fig.2), pentacles - SN 2007gh (Fig.3), stars - Sun spots (Fig.4, left) and triangles - V425 Cas (Fig.4, right). The line $D_1 = D_2$ in the top part is drown by the shortest dashes.

dense enough, we omit the minute range. Figure 6 juxtaposes the derived fractal dimensions D_1 vs. D_2 or $D_2 - D_1$ vs.D_1 for the flickering of KR Aur, collected in Tables 3 and 4, as well as fractal dimensions of the already regarded examples. On the diagram $D_1 - D_2$ (Fig.6, top) we distinguish 4 sequences or data points, corresponding to the flickering in high-state minute-scale (HM, 20 data points), high-state hour-scale (HH, 20 data points), low-

state minute-scale (LM, 6 data points) and low-state hour-scale (LH, 9 data points). These sequences are presented also by regression lines.

Note that in Fig. 6, top, all flickerings are located to the right-down from the line $D_1 = D_2$, typically $D_1 < D_2$. The reason is the defficiency of large single fluctuations, like in the case of random process with uniform distribution with respect to the normal random process (Fig.2, Fig.6, top – filled squares).

In Fig.6, top-left, the sequence HH is situated close to the diagonal line $D_1 = D_2$. The fits of the other sequences deviate significantly from the diagonal, resting almost parallel to it. Hence, the sequences HM and HH are distinct. The sequences LM and LH are poorly presented and are not well distinct.

The design of Fig.6, bottom, resembles color-magnitude in astronomy. It separates the sequences, found in Fig.6, top, better but the vertical standard errors are about two times larger. We consider that diagrams of the type (D_2-D_1) - D_1 might be very useful in case of fractal dimensions derived with high accuracy.

Generally, the fractal plots presented in the Appendix and in Table 3 and 4, as well as the fractal dimensions, compared in Fig.6, give evidences for a significant difference between the minute-scale and hour-scale flickering. This difference may be seen in all photometry bands, as well as in both high and low state. Concretely, on the minute scale D_1 is low and $D_2 - -D_1$ is high compared to the hour scale. Obviously, this is due to a deficiency of strong fluctuations (big jags) on the minute scale and the increase of the amount of the strong fluctuations at large time-scales.

Note also that the dividing time between the minute-time and hour-time scales, adopted here to be 30 min, fluctuates and sometimes it is poor pronounced. More powerful process dominates on the hour-time scale, producing long-lasting brightness increases (flares) and vise versa for the minute time-scale. A set of relatively strong and long increases of the light emission. The less powerfull process dominates in the minute-time scale, producing a set of fainter and shorter increases of the light emission.

So, the **first main result** of the present study is that the flickering of KR Aur, in all states and in all photometry systems, is at least bi-fractal, with dividing time-scale about 30 min. Therefore, at least two physical processes cause the complicated appearance of the flickering process. We note also that the fractal dimensions and their defining time intervals vary moderately in the tine scales from days to years. Consequently, the time scales and the powers of the physical processes that cause the flickering vary moderately.

The third fractal parameter here, H_3, give evidence that sometimes the flickering is like to a periodic process with a period 40 or 80 min. The minima at about log H_3=1.6, corresponding to a period of about 40 min, are well expressed in the observations on Dec 28 and 29, 2010 (No. 122B, 102V, 13V, 14R, 112I, 16I high state). However, such quasi periods are absent in the observations on Dec 30 and 31, 2010 and in other cases. The minima at about log H_3=1.9, corresponding to a period of about 80 min, seem to be present in the observations on Jan 20, 2009 (No. 7U, 6B, 5V, 4R, low state), but they are absent in other cases.

4 Influence of the observing conditions on the fractallity

The present study is based on nonuniform observing material and it is important to elucidate the influence of different circumstances on the derived fractal dimensions.

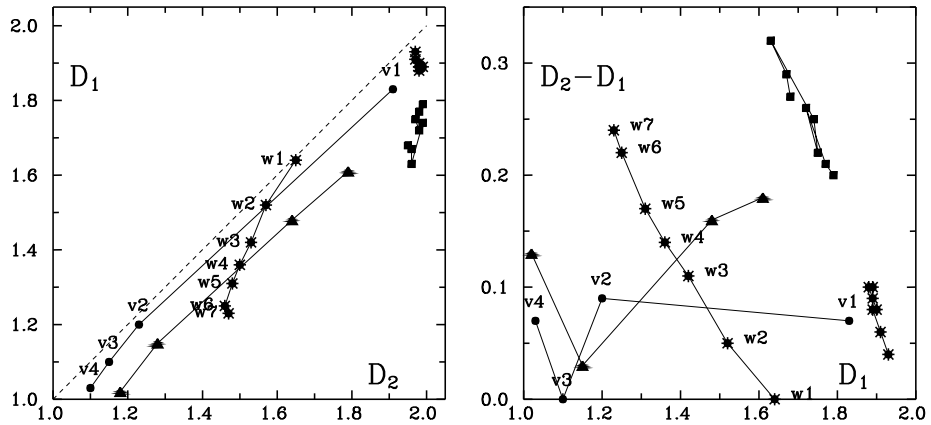

Fig. 7. Trecks of the positions of some time series, used here, after 1,2,3,... time reduction, corresponding to observations with 1,2,3,... larger exposures and 1,2,3,... larger time intervals between the exposures: Squares – uniform random process, Sun signns – year and decade solar activity, Dots – flickering No.V14, Triangles – flickering of V 425 Cas. The treks are directed generally to left-down in the left diagram and left-up in the right diagram, like the prononuced sequences in Fig.6

First, we must explain the appearance of sequences of the fractal diagrams in Fig.6. The real light curve of the flickering is the result of a special type of smoothing, which may be called "exposure transform". This transform averages the signal in the exposure time, producing one data point and omits any signal between exposures. Such transform causes generally left-down shift of the original flickering on the diagram D_1 – D_2 (Fig.6, left) and left-up shift on the diagram (D_2-D_1) – D_1 (Fig.6, right).

Figure 7 shows the effects of consecutive 1,2,3,... times reducing (averaging) of some data rows, that simulates decrease the time resolution and increase of the smoothness of the data. We show the results of applying such transforms as treks of data poins on the fractal diagrams. THe respectie behaviour of 4 time series are shown in Fig.7 - uniform random process, Wolf's numbers of the solar spots, flickering No. V14 and flickering of V425 Cas. These treks explain the appearance of the sequence on the fractal diagrams, shown in Fig.6. Note also that the applied *artificial reduction* decreases stronger D_1 than D_2, because it suppresses the sharp jags more than the standard deviations.

Generally, the decreasing of the fractal dimensions due to the exposure transform may be subject of a special study. Hence, we consider this effect

not to be significant here and use efficiently the fractal diagrams, introduced in Fig.6.

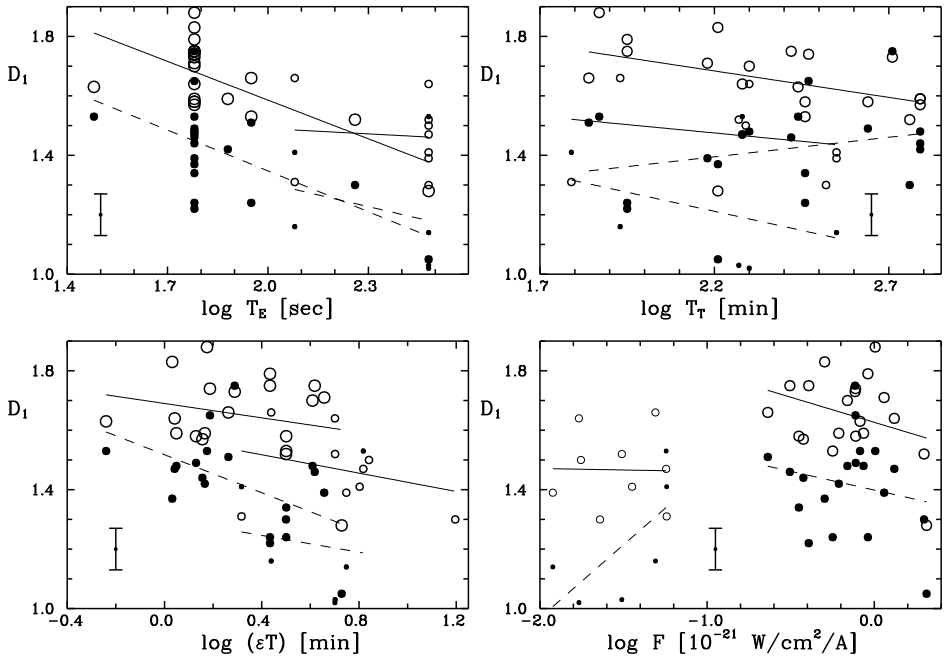

Fig. 8. Influence of the single exposure time T_E, mean time interval between two neighbour exposures ϵT, total observing time T_T and mean flux of KR Aur F on the fractal dimension D_1. The signs of the flickerings and the presentations of the regression lines are the same as in Fig.6.

Further, in Fig.8, we juxtapose the fractal dimension D_1 with 4 parameters of the flickering - exposure time, time interval between the central moments of two consecutive exposures, total observing time of the flickering and flux of the system. It is obvious that only faint correlations exists and the increase of these parameters in majority of cases decrease the fractal dimension with 0.1–0.2. We consider that these changes are relatively small and they do not restrict the application of the fractal analysis.

Note that the scatter of the data in Fig.8, right-bottom is very large. For this reason the fractal dimensions, derived in this work, can not be used as indicators of the energy state of the system.

Our preliminary check shows that an addition of normal noise, like the photometric noise, does not affect considerably the fractal characteristics of the investigated light curve. Hence we avoid the shortest and largest time-scales and estimate the fractal dimensions for intermediate tome-scales.

5 The flickering on the energetic diagrams log F – log H

The fractal plots, corresponding to the equation (3), can characterize the relative energy ΔF of the flickering through the values of the parameters H_1 and H_2 at a given time scale δT. We chose $\delta T_1 = 10$ min for the minute-scale and $\delta T_2 = 100$ min for the hour-scale. Figure 5 illustrates the estimation of the values log $H_{1,1}$, log $H_{2,1}$, log $H_{1,2}$ and log$H_{2,2}$. The solid regression lines in Fig.9 show the anti correlations between these values and the mean flux of KR Aur. The data are collected in Table 3 and 4.

The dashed regression lines in Fig.9 show the local correlation of the compared data. The local horizontal distribution of the fluxes F follows well the energy, corresponding to the respective photometry band. The I-points are situated in the most left parts and the U-points are in the most right parts. However, the scatter is large and these (local) diagrams can not be used for characterizing the energy state of the system.

More important is the general tendency of increasing of the relative energy of the flickering with the decreasing of the energy state of the system. The diagrams in Fig.9 give possibility to compare the powers of the flickering in high and low state.

Let assume that the logarithmic difference between the high and the low states is 2 (from 0 to -2, or 100 times in linear scale or 5 mag). Then the parameters log $H_{1,1}$, log $H_{2,1}$, log $H_{1,2}$ and log $H_{2,2}$ show that in the low state the logarithmic difference is about 0.5. This means that the relative energy of the flickering is about 3 times higher and the absolute energy is $100/3 \approx 33$ times lower, compared to the higher one. Having in mind the "exposure transform" of the data, where the observations in low state are carried out with five times larger exposures, we conclude that these values are lower and higher limits, respectively.

Therefore, the **second main result** of this study, considering the diagrams, shown in Fig.9, is that the flickering energy seems to depend weakly on the energy state of the KR Aur system. Hence, in the low state the relative energy of the flickering is significantly higher than in the high state.

6 Summary of the results

We analyzed 29 light curves of the cataclysmic variable KR Aur, obtained from UBVRI CCD observations with 4 telescopes. The main results are:

1. We tested and established the usefulness of three fractal characteristics of the time series, corresponding to the flickering curves: two for deriving fractal dimensions D_1 and D_2, characterizing the amplitudes and RMS-deviations of the light fluctuations, and one for revealing periodicity in the data series.

2. We found out that the majority of the fractal plots (given in the Appendix) are convex shaped, which is an evidence for least bi-fractal phenomenon, i.e. at least two physical processes are responsible for the observing flickering. One of them dominates in the minute time-scale (adopted here to be 7-30 min) and another dominates in the hour time-scale (adopted here to be 30-300 min). The boundary time scale of 30 min is not well fixed and this is an evidence that the parameters of the physical processes vary moderately.

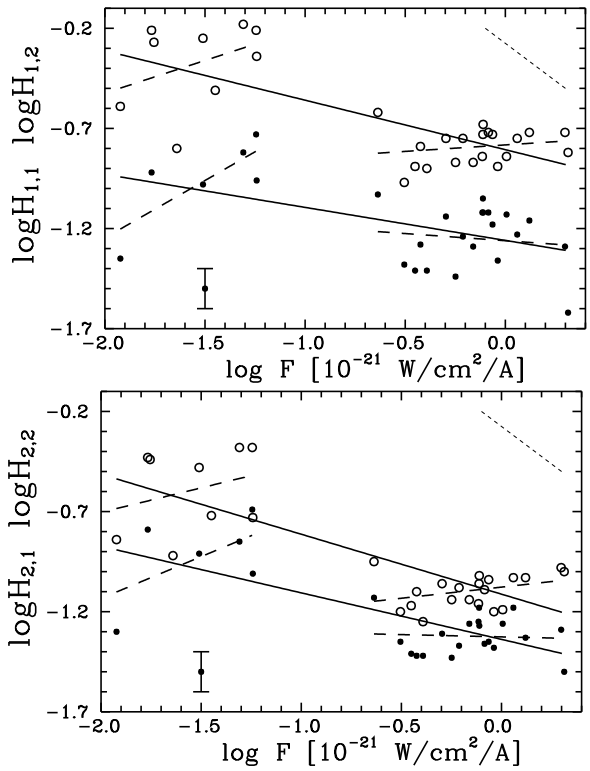

Fig. 9. Increase of the relative energy of the light variations with decreasing of the mean flux of KR Aur, derived from the plots of H_1 (top) and H_2 (bottom), at the points of T=100 min (circles, upper solid lines) and 10 min (dots, down solid lines). Dashed regression lines show the local trends for low state (left) and high state (right). Dotted lines have a slope coefficients of -1 and correspond to the case of flickering, which is independent on the mean flux.

3. We found out that in the case of KR Aur the typical fractal dimensions of the flickering curves are 1.2-1.9 for D_1 and 1.5-1.9 for D_2. The accuracy of our fractal dimension estimates is about 5% (Tables 2,3,4).

4. We use estimations of both fractal dimension in minute and hour time scale to build fractal diagrams (Fig.6). We show that in respect to the minute-scale flickering the hour-scale flickering shows larger in time and stronger by amplitude light fluctuations.

5. Sometimes the flickering show periodicity. For example, on Dec 28 and 29, 2010, in high state, we found 40 min period. However, on Dec 30 and 31, 2010, such periodicity is absent.

6. We show that the "exposure transform" of the flickering causes elongations of the groups HM, HH, LM and LH (Section 3) and forms sequences on the fractal diagrams (Fig.7). Other observational circumstances have not significant influence on the derived fractal dimensions (Fig.8).

7. The flickering of KR Aur in low state is rather powerful. While the common emission flux decreases about 100 times, the relative power of the flickering increases about 3 times ()the absolute power of the flickering decreases not 100 but 33 times). However, the true flickering in the low state is suppressed by the observational "exposure transform" of the large exposures, and really it may be more powerful than estimated here.

8. The values of the fractal dimensions D_1 and D_2, as well as the values of the fractal parameter H_1 and H_2 at chosen time scales, can not be used as indicators of the energetic state of the system (Fig.8, right-bottom, and Fig.9).

Acknowledgements

The authors would like to thank Radoslav Zamanov and Vasil Popov for the assistance and worth recommendations about this paper.

This work has been partially supported by the Bulgarian National Research Fund through grants DO 02-85 and BIn 13/09.

References

Bachev R., Boeva S., Georgiev Ts., Latev G., Spassov B., Stoyanov K., Tsvetkova S.,2011, *Bulg.Astron.J.* 16
Bessell M.S., 1979, *PASP* 91, 589
Boeva S.,Zamanov R.K., Antov A., Bachev R., Georgiev Ts.B., 2007, *Bulg.Astron.J.* 9, 11-16
Boeva S., Antov A., Bachev R., 2010, *Bulg.Astron.J.* 13, 40-46
Dimitrov.D., Kyurkchieva D., Danailova M., 2011, *Bulg.Astron.J.* 15, 57-63
Falconer K., 1997, *Techniques in Fractal Geometry*, John Willey & Sons
Hastings H.M., Sugihara G., 1995, *Fractals. A user guide for Natural Sciences*, Oxford University Press.
Hunter D.J., et al., 2009, *Astro.Astrophys.* 508, 371-389
Mandelbrot B.B., 1982, *The fractal Geometry of Nature*, Freeman, New York
Peitgen H.-O, Jurgens H., Saupe D., 1992, *Chaos and Fractals*, Springer-Verlag
Popova M., 1965, *Peremen. zvjozdy* 15/4, 534
Russ J.C., 1994, *Fractal Surfaces*, Plenum Press, New York & London
Shafter A.W., 1983, *ApJ*, 267, p 222
Tsvetkova S., Boeva S., 2009, *Bulg.Astron.J.* 12, 43-47

Table 1. Basic data about the observations: 1 - Sign and photometry band; 2 - Date; 3 - Telescope (sh - Schmidt in Rozhen, cr - Cassegrain in Rozhen, cb - Cassegrain in Belogradchik, 2m - 2 m in Rozhen); 4 - Number of exposures; 5 - Single exposure time, in seconds; 6 - Mean separate time between the central moments of the neighbor exposures, in minutes; 7 - Total observing time, in hours; 8,9,10 - Average, RMS and Amplitude (MAX-MIN) of the light curve; 11 - Mean light flow of the light curve, expressed in units of 10^{-21} W/A/cm^2 through Bessel's (1979) constants.

#	Date	Tel	n_E	t_{EXP}	t_{SEP}	t_{TOT}	m_0	m_S	m_A	lgF
1	2	3	4	5	6	7	8	9	10	11
	Observations in the high state of the system									
16U	30.12.2010	sh	180	180	3.2	9.5	13.33	0.18	0.79	0.300
20U	31.12.2010	2m	30	300	5.5	2.8	13.28	0.14	0.45	0.314
121B	29.12.2010	sh	50	90	1.5	2.3	14.54	0.08	0.33	-0.060
122B	29.12.2010	cr	33	120	4.6	2.5	14.40	0.10	0.40	0.060
21B	31.12.2010	sh	170	60	1.1	3.2	14.26	0.11	0.48	0.120
102V	28.12.2010	cb	36	90	2.5	1.2	13.99	0.07	0.39	-0.038
13V	29.12.2010	2m	110	60	2.4	4.4	14.25	0.09	0.42	-0.144
17V	30.12.2010	2m	549	60	1.1	9.8	14.06	0.15	0.68	-0.064
22V	31.12.2010	2m	475	30	0.6	4.5	14.11	0.11	0.55	-0.085
27V	03.03.2000	2m	38	90	1.9	1.2	15.48	0.12	0.48	-0.635
14R	29.12.2010	cb	152	60	1.1	2.7	14.13	0.10	0.42	-0.297
18R	30.12.2010	cr	312	60	2.7	8.1	13.92	0.13	0.58	-0.212
23R	31.12.2010	cr	91	90	3.2	4.8	14.01	0.10	0.40	-0.249
5I	28.01.2006	cb	213	60	1.9	8.6	13.12	0.09	0.50	-0.115
6I	29.01.2006	cb	194	60	1.5	8.5	13.00	0.11	0.49	-0.112
9I	11.01.2007	sh	326	45	1.4	7.3	13.00	0.12	0.63	-0.111
112I	28.12.2010	cb	36	60	2.6	1.5	13.70	0.06	0.24	-0.393
15I	29.12.2010	cr	63	60	4.2	4.4	13.98	0.07	0.29	-0.505
19I	30.12.2010	cr	434	60	1.3	9.9	13.79	0.14	0.56	-0.424
24I	31.12.2010	cr	90	90	3.2	4.8	13.85	0.09	0.39	-0.451
	Observations in the low state of the system									
2U	26.02.2009	2m	47	300	6.4	6.1	17.70	0.22	0.93	-1.446
7U	20.01.2009	2m	26	300	7.5	3.4	17.25	0.40	1.42	-1.232
1B	26.02.2009	sh	21	300	5.9	5.7	18.66	0.35	1.33	-1.642
6B	20.01.2009	sh	37	300	5.2	3.3	18.39	0.35	1.33	-1.510
3V	26.02.2009	2m	60	300	6.0	6.1	18.71	0.15	0.68	-1.927
5V	20.01.2009	2m	35	300	5.6	3.3	18.35	0.33	1.27	-1.761
25V	20.03.1999	2m	31	120	2.8	1.5	17.23	0.36	1.21	-1.314
26V	03.12.1999	2m	30	120	2.1	1.1	17.01	0.15	0.67	-1.243
4R	20.01.2009	cb	40	300	5.0	3.4	17.87	0.39	1.41	-1.762

Table 2. Data about the fractal dimensions D_1 and D_2, and their standard errors σ_{D1} and σ_{D2} for the examples, shown in Fig.2 – Fig.5

Figure and its contents	D_1	σ_{D1}	D_2	σ_{D2}
Fig.2, SN 2007 gh, B-mag	1.21	0.05	1.28	0.04
Fig.2, SN 2007 gh, (B-V)	1.44	0.05	1.59	0.06
Fig.3, Gaussian random numbers	1.79	0.02	1.99	0.00
Fig.3, Uniform random numbers	1.96	0.02	2.00	0.00
Fig.4, Wolf number, 1-10 years	1.64	0.05	1.65	0.02
Fig.4, Wolf number,10-46 years	1.93	0.02	1.97	0.02
Fig.4, V 425 Cas, 2-7 minutes	1.53	0.03	1.68	0.03
Fig.4, V 425 Cas, 7-40 minutes	1.61	0.03	1.79	0.03
Fig.5, KR Aur B, minute scale	1.47	0.05	1.70	0.02
Fig.5, KR Aur B′, minute scale	1.53	0.04	1.69	0.02
Fig.5, KR Aur B, hour scale	1.64	0.05	1.70	0.04
Fig.5, KR Aur B', hour scale	1.65	0.05	1.70	0.04

Table 3. Data about the flickering of KR Aur in the minute scale (7-30 min)

#	D_1	σ_{D1}	lg $H_{1,10}$	D_2	σ_{D2}	lg $H_{1,10}$	log F
			High state				
16u	1.30	0.08	-1.29	1.69	0.05	-1.29	0.298
20u	1.05	0.18	-1.62	1.52	0.09	-1.50	0.313
121b	1.53	0.06	-1.13	1.89	0.04	-1.26	0.006
122b	1.39	0.09	-1.23	1.77	0.10	-1.18	0.059
21b	1.47	0.05	-1.16	1.70	0.02	-1.33	0.120
102v	1.24	0.20	-1.36	1.61	0.11	-1.38	-0.038
13v	1.48	0.17	-1.29	1.81	0.13	-1.26	-0.161
17v	1.48	0.03	-1.18	1.70	0.01	-1.35	-0.064
22v	1.53	0.03	-1.12	1.72	0.02	-1.36	-0.085
27v	1.51	0.06	-1.03	1.84	0.03	-1.13	-0.637
14r	1.37	0.03	-1.14	1.59	0.02	-1.31	-0.297
18r	1.42	0.03	-1.24	1.68	0.02	-1.37	-0.212
23r	1.24	0.12	-1.44	1.69	0.06	-1.43	-0.249
112i	1.22	0.20	-1.41	1.63	0.11	-1.42	-0.392
15i	1.46	0.06	-1.38	1.79	0.04	-1.35	-0.505
19i	1.44	0.03	-1.28	1.72	0.01	-1.42	-0.424
24i	1.34	0.10	-1.41	1.76	0.04	-1.41	-0.451
05i	1.75	0.06	-1.12	1.90	0.03	-1.25	-0.115
06i	1.65	0.04	-1.05	1.87	0.02	-1.18	-0.112
09i	1.49	0.05	-1.12	1.69	0.03	-1.27	-0.111
			Low state				
07u	1.53	0.37	-0.73	1.73	0.37	-0.69	-1.245
06b	1.03	0.16	-0.98	1.38	0.11	-0.91	-1.510
03v	1.14	0.16	-1.35	1.38	0.12	-1.30	-1.923
25v	1.16	0.08	-0.82	1.52	0.11	-0.85	-1.309
26v	1.41	0.05	-0.96	1.77	0.04	-1.01	-1.242
04r	1.02	0.55	-0.92	1.53	0.25	-0.79	-1.767

Table 4. Data about the flickering of KR Aur in the hour scale (30-300 min)

#	D_1	σ_{D1}	lg $H_{1,100}$	D_2	σ_{D2}	lg $H_{1,100}$	log F
			High state				
16u	1.52	0.04	-0.72	1.65	0.03	-0.98	0.298
20u	1.28	0.05	-0.82	1.41	0.06	-1.00	0.313
121b	1.88	0.07	-0.84	1.96	0.11	-1.19	0.006
122b	1.71	0.11	-0.75	1.94	0.03	-1.03	0.059
21b	1.64	0.05	-0.72	1.71	0.04	-1.03	0.120
102v	1.79	0.07	-0.89	2.01	0.04	-1.20	-0.038
13v	1.70	0.04	-0.87	1.94	0.03	-1.14	-0.161
17v	1.59	0.02	-0.73	1.66	0.03	-1.04	-0.064
22v	1.63	0.03	-0.72	1.68	0.05	-1.09	-0.085
27v	1.66	0.13	-0.62	1.80	0.08	-0.95	-0.637
14r	1.83	0.03	-0.75	1.91	0.02	-1.06	-0.297
18r	1.59	0.01	-0.75	1.70	0.01	-1.08	-0.212
23r	1.53	0.02	-0.87	1.65	0.06	-1.14	-0.249
05i	1.73	0.02	-0.84	1.94	0.02	-1.16	-0.115
06i	1.74	0.02	-0.73	1.89	0.02	-1.06	-0.112
09i	1.58	0.01	-0.68	1.76	0.02	-1.02	-0.111
112i	1.75	0.12	-0.90	2.00	0.05	-1.25	-0.392
15i	1.75	0.02	-0.97	1.92	0.02	-1.20	-0.505
19i	1.57	0.01	-0.79	1.63	0.02	-1.10	-0.424
24i	1.58	0.02	-0.89	1.68	0.06	-1.17	-0.451
			Low state				
02u	1.41	0.07	-0.51	1.71	0.08	-0.72	-1.449
07u	1.47	0.07	-0.21	1.73	0.08	-0.38	-1.245
01b	1.30	0.10	-0.80	1.70	0.09	-0.92	-1.641
06b	1.52	0.07	-0.25	1.76	0.08	-0.48	-1.510
03v	1.39	0.06	-0.59	1.71	0.05	-0.84	-1.923
05v	1.50	0.06	-0.27	1.73	0.06	-0.44	-1.755
25v	1.66	0.14	-0.18	1.70	0.16	-0.38	-1.309
26v	1.31	0.12	-0.34	1.65	0.15	-0.73	-1.242
04r	1.64	0.11	-0.21	1.83	0.09	-0.43	-1.767

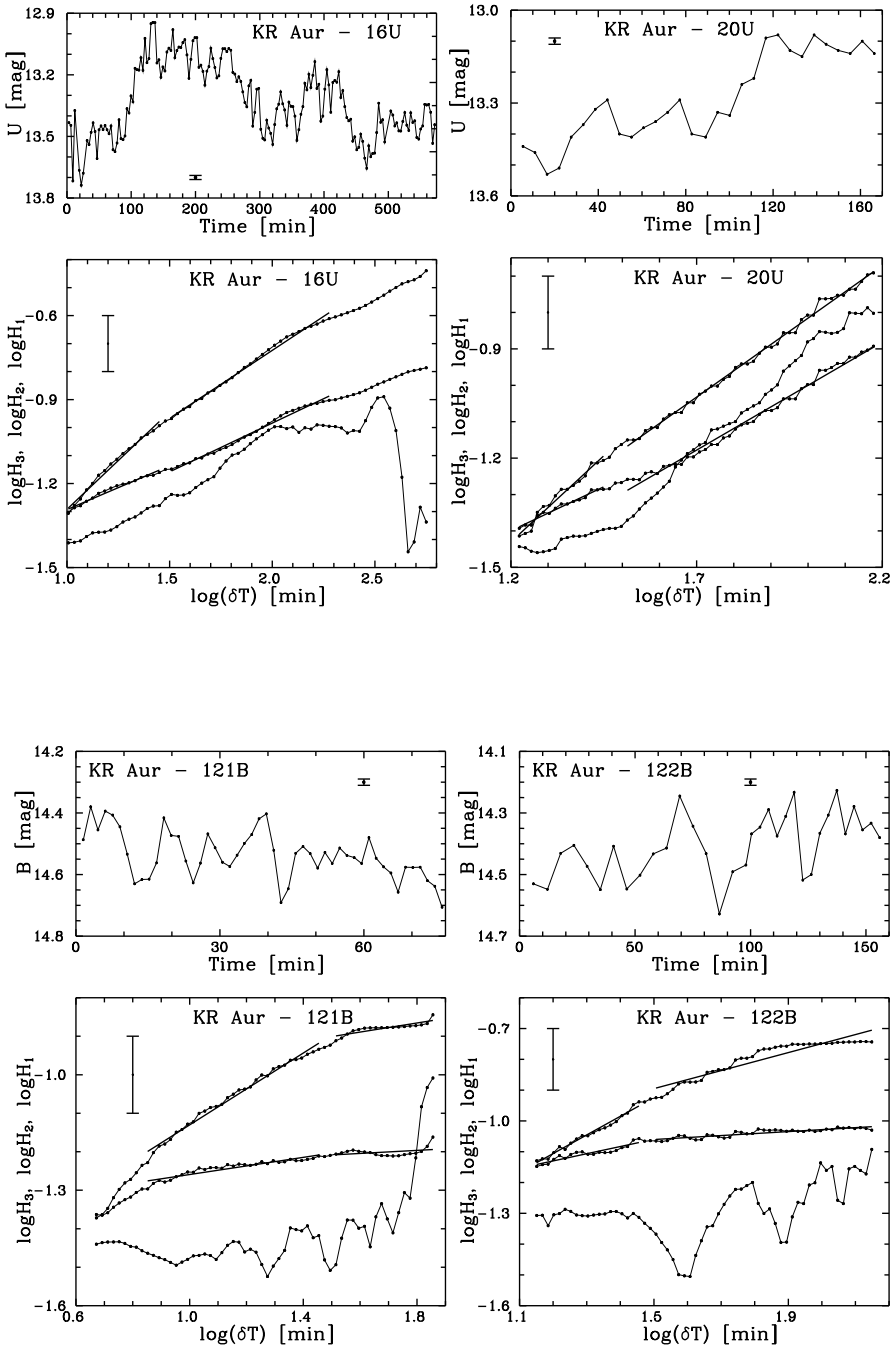

Fig. 10. KR Aur in the high state

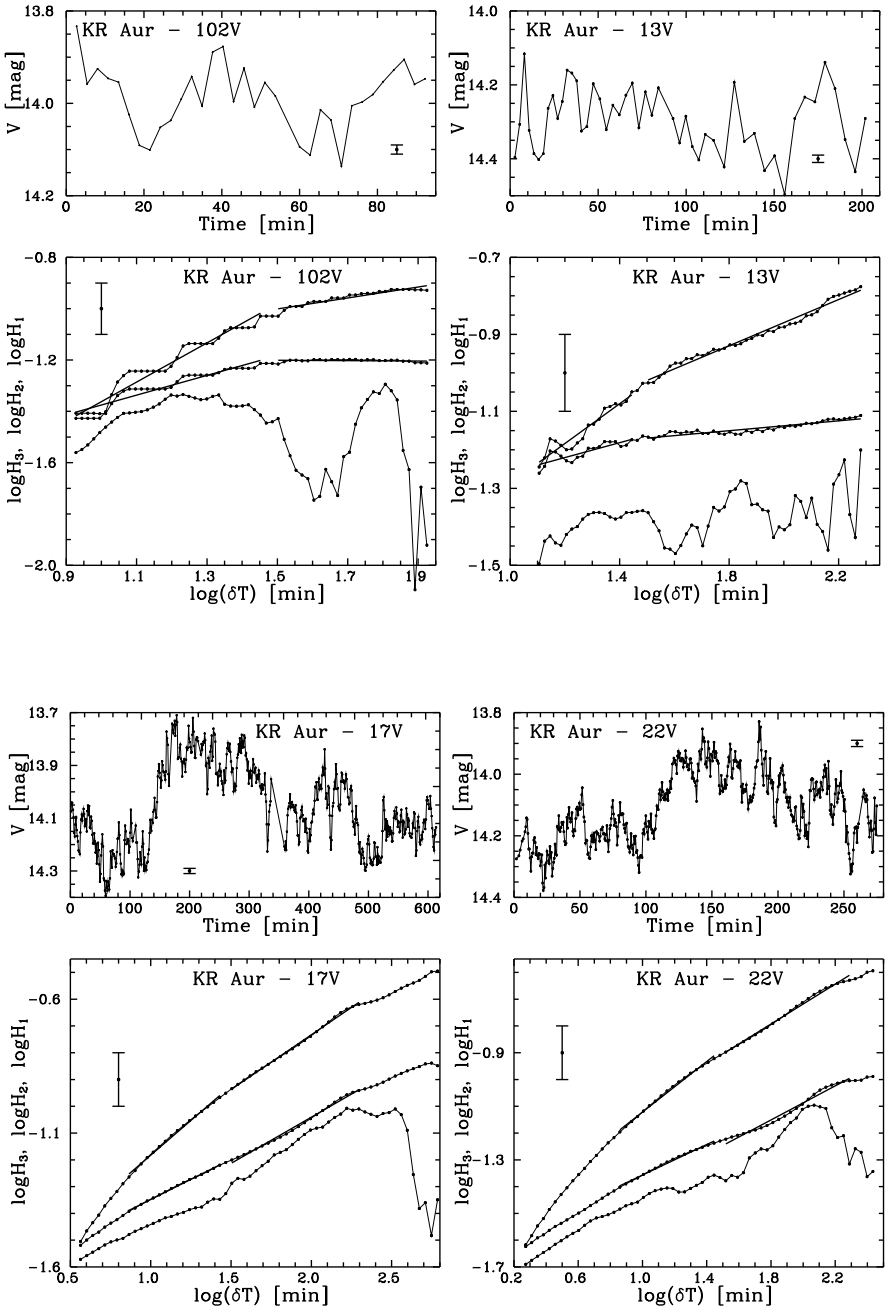

Fig. 11. KR Aur in the high state

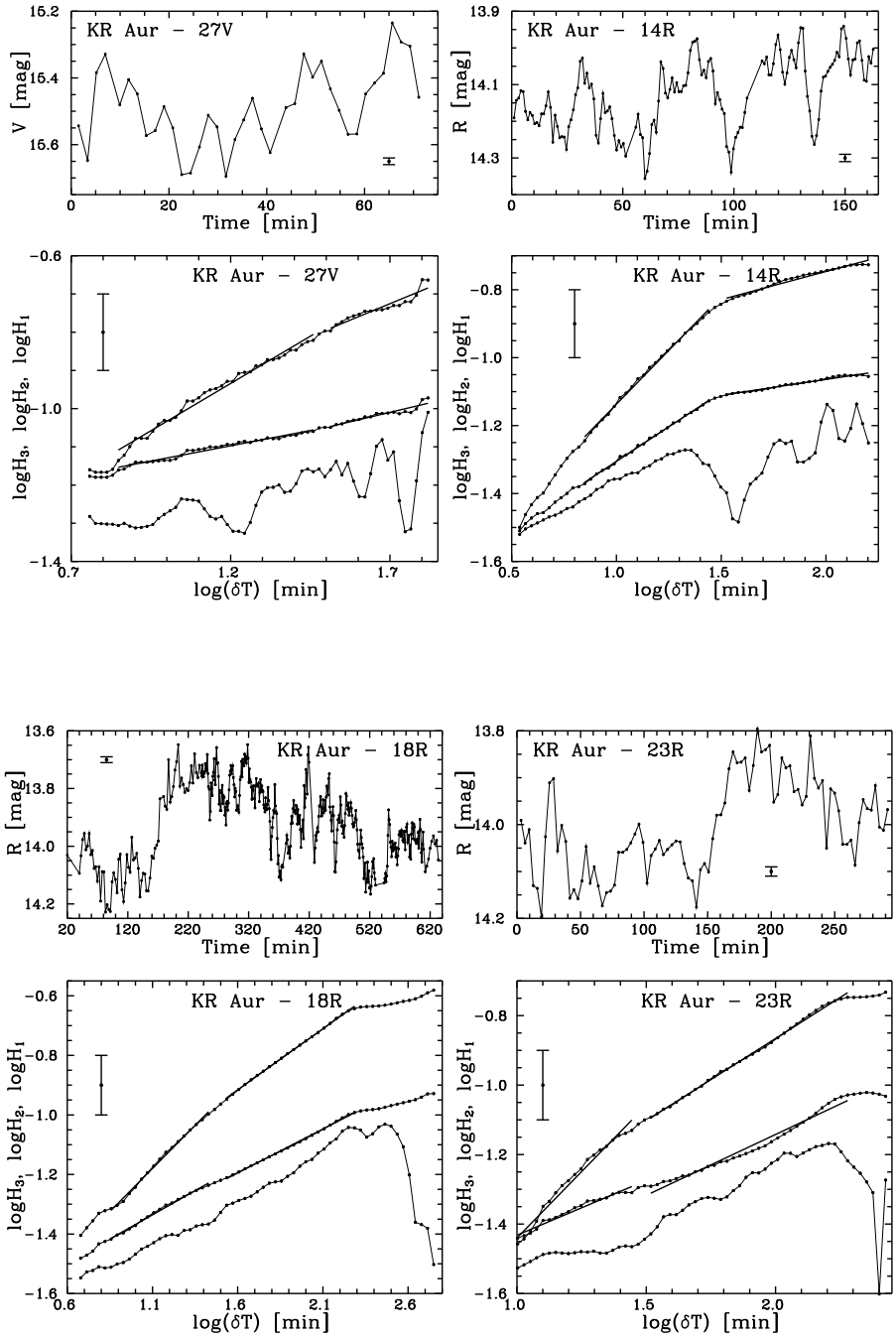

Fig. 12. KR Aur in the high state

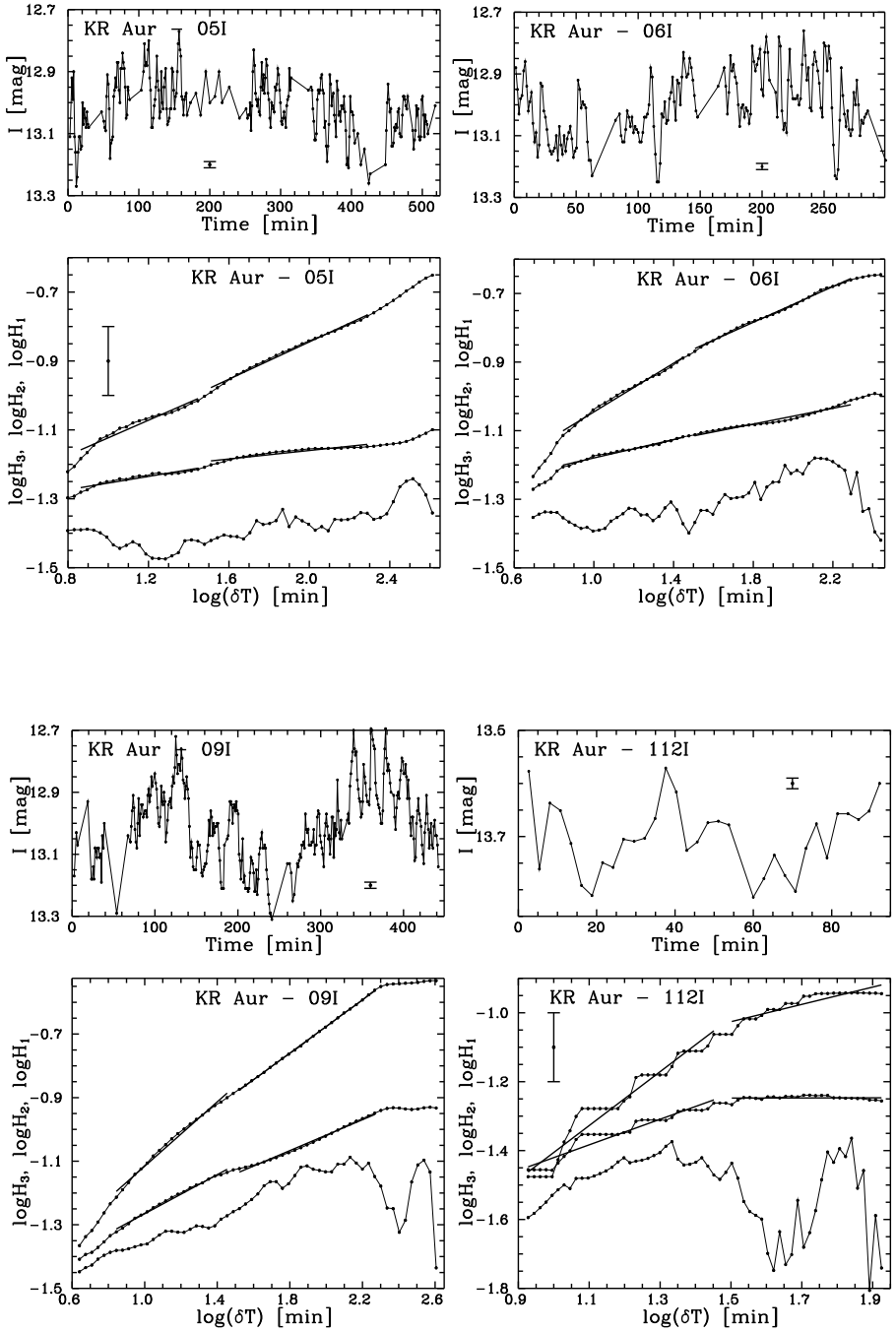

Fig. 13. KR Aur in the high state

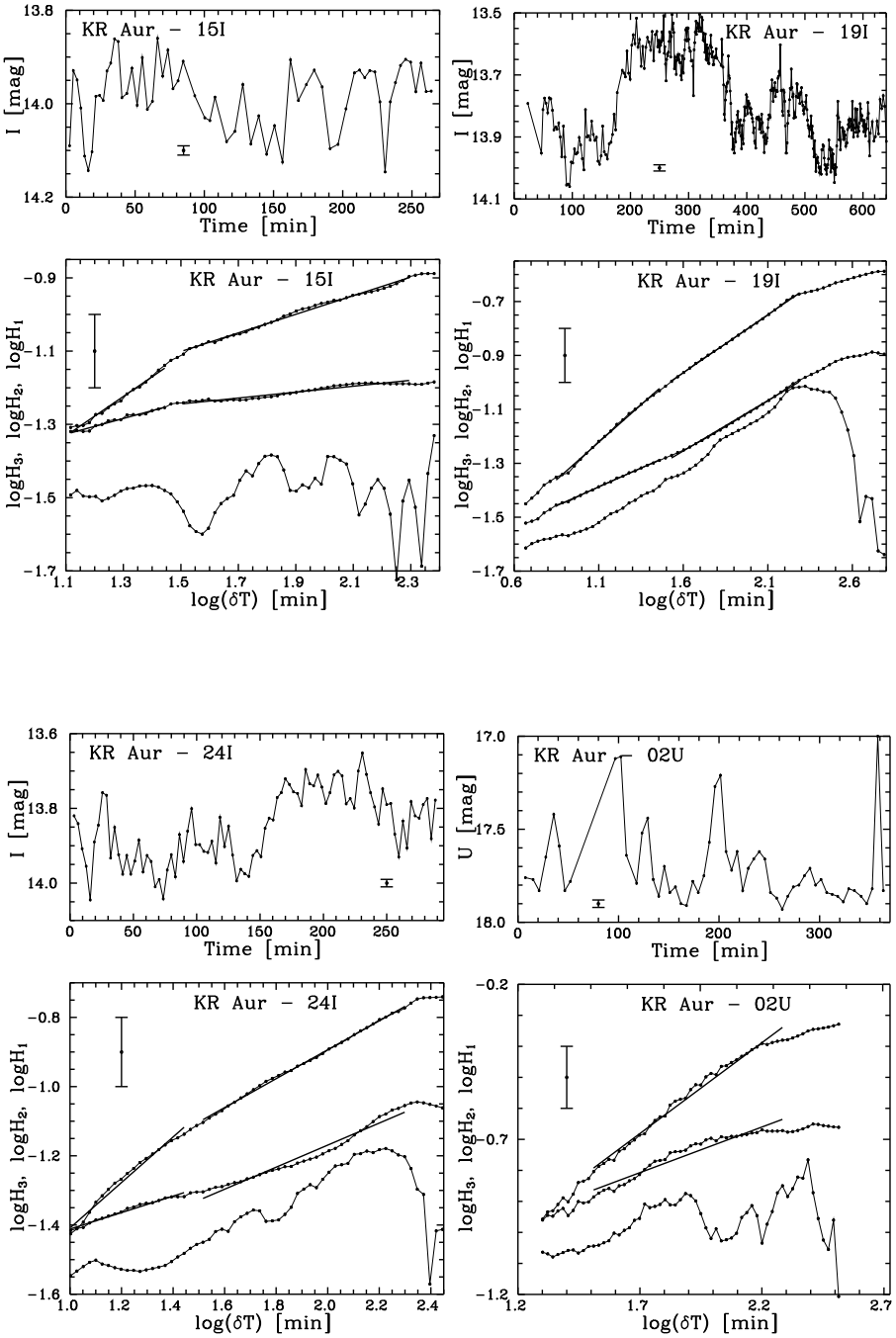

Fig. 14. KR Aur in the high state (15I,19I,24I) and in the low state (02U)

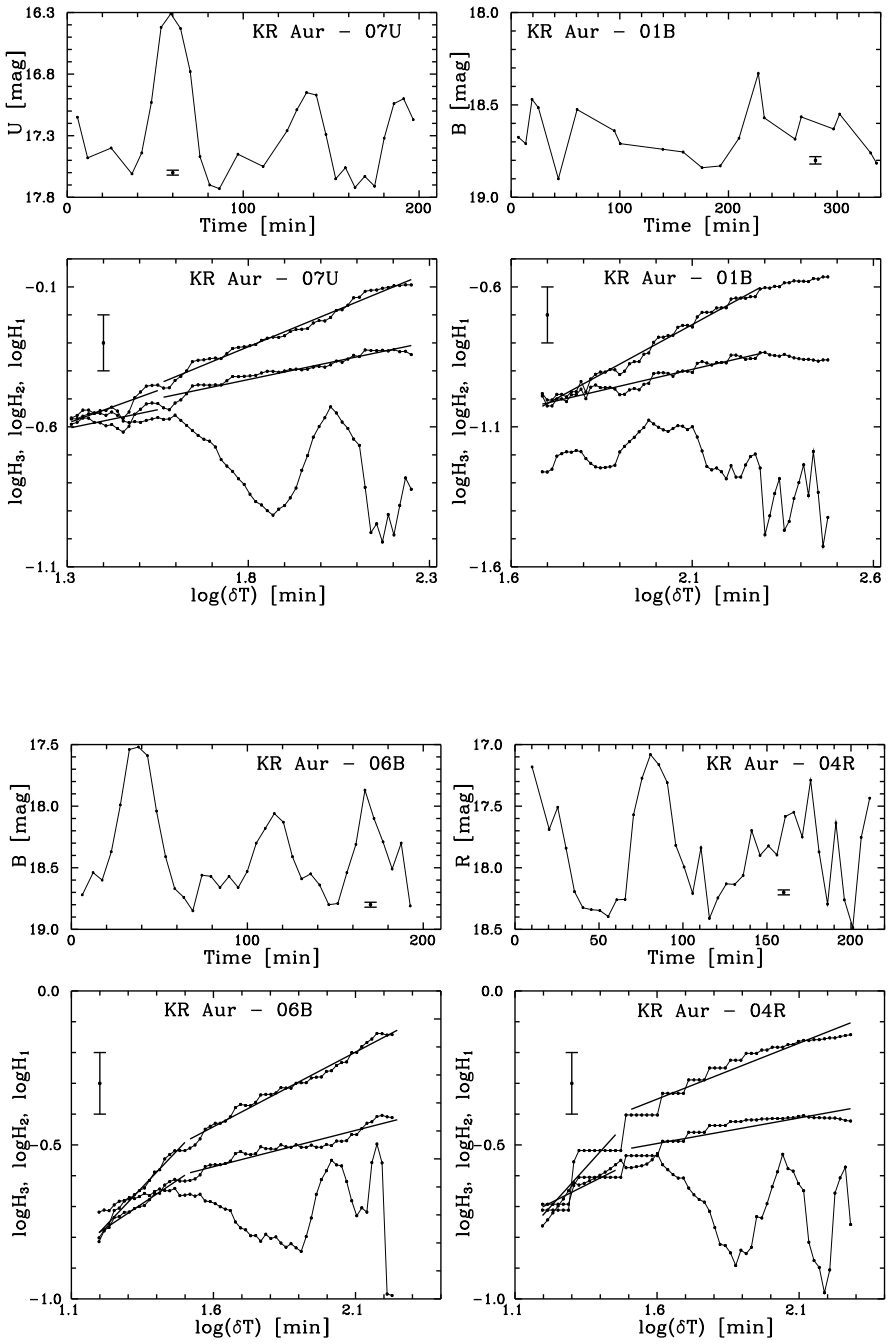

Fig. 15. KR Aur in the low state

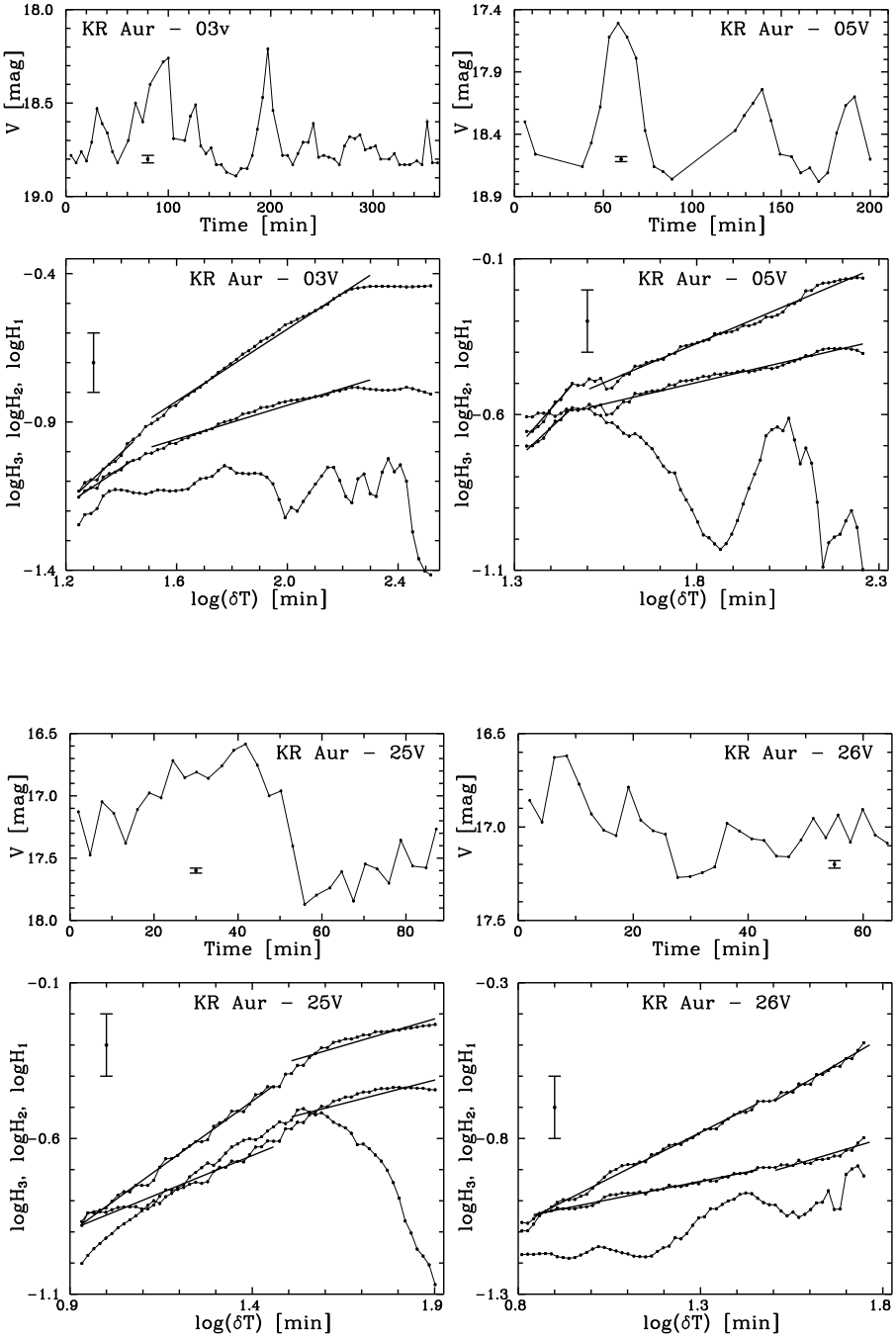

Fig. 16. KR Aur in the low state